Available online at www.sciencedirect.com
ScienceDirect
Journal of Colloid and Interface Science 317 (2008) 166–174
JOURNAL OF Colloid and Interface Science
www.elsevier.com/locate/jcis

Study of Ni–Ag/SiO_2 catalysts prepared by reduction in aqueous hydrazine

R. Wojcieszak, S. Monteverdi, J. Ghanbaja, M.M. Bettahar *

UMR 7565, Catalyse Hétérogène, Faculté des Sciences, Université Henri Poincaré, Nancy-I BP 239, 54506 Vandoeuvre-lès-Nancy Cedex, France

Received 21 June 2007; accepted 13 September 2007

Available online 18 September 2007

Abstract

We have studied bimetallic Ni–Ag (Ni + Ag = 1 wt%) catalysts supported on crystallized silica and prepared by aqueous chemical reduction with hydrazine at 353 K. Two protocols of reduction were used. Prepared catalysts were characterized by means of XRD, TEM, STEM, H_2 chemisorption and H_2-TPD. Their catalytic activity was studied in the gas-phase hydrogenation of benzene. The most important feature of the results obtained is the synergistic effect between Ni and Ag which led to improvement of dispersion and reactivity of nickel in the presence silver for precipitated catalysts. Silver is inactive in the test-reaction. Precipitated bimetallic catalysts give rise to total conversion from 373 K, a temperature at which conversion hardly reaches 30% for the impregnated catalysts. Dispersion and activity pass through a maximum of monotonically decrease with precipitated and impregnated catalysts, respectively. Deactivation was observed for bimetallic catalysts, particularly with precipitated samples. These results could be explained by the mechanism of metal reduction in the hydrazine media. As a result, various Ni–Ag species formed where Ni and Ag phases were separated clusters or interacted as heteroatomic groupings on the carrier surface. These grouping would be responsible of the high performances of the precipitated catalysts.

Keywords: Supported bimetallic catalysts; Nickel; Silver; Silica; Hydrazine; Benzene hydrogenation

1. Introduction

Nanoparticles of transition or noble metals have attracted much attention because of their unusual properties compared with the conventional polycrystalline materials. Whereas in the macromolecular solid, surface atoms contribute only a relatively small fraction of the total number of metal atoms, the nanoparticles contain almost all surface atoms [1]. It follows that such atoms have lower coordination numbers than in the bulk and as a consequence are expected to exhibit greatly enhanced activity to all manner of substrates [1]. The synthesis of metal nanoparticles has been focus of numerous studies in the last decade. Some very successful techniques have been developed for producing gold [2–4], silver [5–7], nickel [8–12], platinum [13], copper [14] and other materials as nanoparticles.

Recently, increasing interest has been shown in preparing metal alloys such as Au/Pd [15], Au/Pt [16], Fe/Ni [17], Ni/Cu [18,19] and Ni/Ag [20–23]. It has been demonstrated that even with small particles bimetallic clusters are vastly superior to their monometallic counterparts [1,15].

Nickel supported catalysts are widely used in heterogeneous catalysis due to their high hydrogenating properties. Many parameters determine its catalytic activity in hydrogenation processes. The activity strongly depends on the nature of the support which may modify the properties of the active phase. The extent of metal–support interaction and support acidity seems to play a crucial role in complex chemistry of nickel supported catalysts [24–27]. Silver supported catalyst is considered as an excellent catalyst in epoxidation and oxidation reaction [28,29]. However, it is not active in the hydrogenation processes. Nevertheless, incorporation of silver to palladium catalysts improves the hydrogenation properties. It was shown that incorporation of silver into palladium catalysts increases their selectivity in the acetylene hydrogenation [30].

Hydrazine is a powerful strong reductant widely used in various chemical operations. A series of striking results has been obtained where hydrazine is used as a reducing agent for the production of finely divided metals [31–36]. Degan and Macek [35] used hydrazine as a reducing agent to prepare nickel powders in the submicrometer size range from nonaqueous solu-

* Corresponding author.
E-mail address: mohammed.bettahar@lcah.uhp-nancy.fr (M.M. Bettahar).

0021-9797/$ – see front matter
doi:10.1016/j.jcis.2007.09.031

tions of nickel salts. The rate and yield of the reaction were both enhanced at higher reaction temperatures but were limited by the relatively low boiling point of water. Nickel powders with mean particle sizes ranging from 0.1 to several μm and with up to 99.8% purity were obtained by this method. Nickel et al. [36] studied the production of a silver colloid by reduction with hydrazine as a support for highly sensitive surface-enhanced Raman spectroscopy. The reduction of aqueous silver nitrate by hydrazine dihydrochloride in weakly alkaline solution results in a polydisperse colloid that is stable for many months without addition of stabilizing compounds. The average size of the predominantly spherical particles depends on the initial concentration of silver ions and ranges from 40 to 70 nm in diameter.

Our group has undertaken a systematic study of nickel metal nanoparticles supported on crystallized silica of low specific surface area, prepared by reduction of nickel acetate by hydrazine in aqueous media [34]. It was shown that the morphology of the particles formed changed with the reduction condition and metal loading. The particle shape obtained influenced their surface and catalytic properties. Incorporation of copper in nickel also gave rise to changes in the particles morphology and surface properties [37]. Indeed, nickel was found in a whisker-like shape in monometallic Ni/SiO_2 and as a film of low density in bimetallic $Ni–Cu/SiO_2$. The Ni particle size is lower than 2 nm in both cases. The copper phase is in the shape of facetted particles in the mono or bimetallic systems with a mean particle size of about 25 nm. The metal dispersion as determined by hydrogen adsorption decreased with the copper content due to Ni–Cu interactions. The amounts of hydrogen incorporated in the catalysts during a previous hydrogen heat treatment changed with the copper content for the same reason.

In the present paper we report the study of 1% nickel–silver supported catalysts prepared by the chemical reduction with hydrazine. Different concentrations of Ag and Ni have been used. Crystallized silica was used as the support for Ni–Ag active phase. The catalysts were characterized by means of XRD, TEM and H_2 adsorption/desorption studies. They were tested in the gas phase hydrogenation of benzene.

Catalytic studies on supported bimetallic Ni–Ag systems have not received much attention. The scarce data reported interestingly show that silver improves the reducibility and the stability of the nickel active phase [38,39]. However, these results are at variance with that reported for unsupported NiAg systems. Indeed, only metastable NiAg alloys have been observed in specific conditions [21,22]. These alloys give rise to phase separation and reformation of Ni and Ag particles with time on stream [21]. Our study aimed to re-investigate this system in preparation conditions not reported before, namely the hydrazine media and using silica as a support. For comparison with previous studies, we used a silica support of low surface area [34]. These studies showed that a silica support of high surface area does not allow nickel reduction in the hydrazine media. Reduction is favoured with basic rather than acidic supports [40].

2. Experimental

2.1. Catalysts

Nickel acetate solution ($Ni(CH_3COO)_2{\cdot}4H_2O$) and silver nitrate solution ($AgNO_3$) were purchased from Fluka (⩽99.0%) and Prolabo (⩽99.0%), respectively. Silica was purchased from Chempur (⩽99.0%, 15 $m^2\,g^{-1}$). Hydrazine water solution (24–26%) was purchased from Merck (⩽99.0%).

Two series of catalysts were prepared.

The first one included materials denoted as IC (Impregnated Chempur) catalysts which were prepared by classical wet impregnation method then reduction in a hydrazine solution. The silica support (5 g) was poured over nickel acetate and silver nitrate solution with the appropriate concentration. After filtration and 15 min of rotation under vacuum, the mixture was heated and evaporated for 1 h. The solid obtained was dried at 383 K for 1 h. The nickel acetate and silver nitrate concentrations in the solution were calculated to obtain the following Ni–Ag ratios: 1.00% Ni, 0.90% Ni–0.10% Ag, 0.75% Ni–0.25% Ag and 0.50% Ni–0.50% Ag, 1.00% Ag.

After impregnation, the catalysts were reduced with hydrazine solution as follows. The preparation was performed under argon atmosphere (flow rate = 100 $cm^3\,min^{-1}$) in a 3 necked reaction flask of 110 cm^3 dipping in a water bath. The reaction flask was fitted with a reflux condenser and a thermocouple for the control of the reaction temperature and connected to a gas microchromatograph (Agilent G2890A) for the analysis of the gases evolved during the reduction process. A suspension of the supported nickel precursor (5 g of impregnated sample in 60 cm^3 of water) was stirred for 20 min at room temperature. The reaction mixture was slowly heated from room temperature up to 353 K. Then 10 ml of 24–26% aqueous hydrazine in excess (>99% Fluka) was added. The pH of the solution was 10–12 and remained almost constant. Reaction was stopped after 4 h. After reduction the solid was filtered and dried in air at 353 K for 5 h. Note that, after impregnation then drying at 383 K in air, no metal ions were detected in the reaction media when a suspension of the precursor was stirred for 20 min.

The second set of catalysts denoted as PC (Precipitated Chempur) was prepared by simultaneous introduction of appropriate concentration of nickel acetate, silver nitrate and 5 g of silica in 60 cm^3 of distilled water in the 3 necked reaction flask. The reactant mixture was heated to 353 K and then 10 cm^3 of hydrazine was added. Reduced precursors precipitated on the support. Reaction was stopped after 4 h. The obtained solid was filtered and dried in air at 353 K for 5 h.

2.2. Characterization of physico-chemical properties

XRD patterns were recorded with a classical $\Theta/2\Theta$ diffractometer using Cu$K\alpha$ radiation. The electron microscopy images were obtained with a Phillips CM20 STEM microscope after placing a drop of the catalyst suspension on the carbon coated copper grid. X-ray microanalysis chemical compositions were determined using energy dispersive X-ray spectroscopy (EDXS). EDXS spectra were recorded by means of an EDAX

spectrometer mounted on the Philips microscope and equipped with an ultra-thin window X-ray detector. The analysis were carried out in nanoprobe mode with a diameter of the probe of 10 nm. The K_{AB} factors were determined using standards.

Previous results [34,40] showed that the supported nickel precursor is highly reduced in the hydrazine media. However, the as-received samples are superficially re-oxidized during the drying in air. Also H_2 chemisorption, H_2-TPD, degree of reduction and catalytic studies were carried out on hydrogen pretreated samples. The pre-treatment was performed in a flow of pure hydrogen (flow rate = 100 $cm^3\,min^{-1}$). 0.1 g of a catalyst was placed in a quartz reactor and heated at a rate of 10 K min^{-1} to 573 K. The sample was heated at 573 K for 2 h. Then, the reduced sample was treated in a flow of argon at the reduction temperature for 1 h (flow rate = 100 $cm^3\,min^{-1}$) and then cooled to room temperature under argon atmosphere for subsequent hydrogen adsorption.

The hydrogen adsorption was carried out using a mixture of H_2/Ar (100 ppm H_2). The reactant gas (100 ppm H_2/Ar) was injected in the reactor and the amount of hydrogen chemisorbed was detected each 2 min. Assuming spherical metal particles, the metal mean size was calculated from the following relation [38]: $d = 971/D$, where D is the metal dispersion as determined by H_2 adsorption. The dispersion was calculated taken into account the fraction of reduced nickel.

H_2 adsorption was followed by H_2-TPD after purging the sample under argon (1 h) then flowing with the same gas (100 $cm^3\,min^{-1}$) in programmed temperature mode up to 1123 K using a ramp of 5 K min^{-1}. The amount of desorbed hydrogen was detected with a thermal conductivity detector in an Agilent G2890A MicroChromatograph.

The degree of reduction was determined according to Ref. [27]. For all the catalysts, the sample was heated at rate of 10 K min^{-1} to 573 K for 2 h and reduced in a flow of hydrogen pure (flow rate = 100 $cm^3\,min^{-1}$). After the reduction, the sample was treated in a flow of argon at the reduction temperature for 1 h with a flow rate of 100 $cm^3\,min^{-1}$. It was again purged at 623 K for 1 h. The oxygen adsorption was carried out using a mixture of O_2/Ar (100 ppm O_2) which was injected to the reactor at 623 K with a flow rate of 100 $cm^3\,min^{-1}$. The quantity of oxygen consumed was detected each 2 min as for hydrogen.

2.3. Catalytic activity

The gas-phase benzene hydrogenation reaction was performed in a quartz reactor equipped with a thermocouple. A 0.1 g of a catalyst was placed in the reactor and it was pretreated in a flow of hydrogen pure (flow rate = 100 $cm^3\,min^{-1}$). After the reduction, carried out 2 h at 573 K after heating with a ramp of 10 K min^{-1}, the sample was cooled to the desirable temperature. Gas mixture containing benzene and H_2 (1 vol% of benzene) was prepared by passage of H_2 stream through a benzene (Merck, >99%) placed in a saturator maintained at 278.4 K. The reactant mixture was passed through the reactor with total flow rate of 50 $cm^3\,min^{-1}$. The catalytic test was carried out at various temperatures on the same catalyst. The sample was heated or cooled at a rate of 10 K min^{-1}. Benzene and the reaction products were analyzed each 6 min with 5730A Hewlett Packard gas chromatograph, operated at a programmed temperature and with a flame ionization detector.

The stability test on reduced samples (0.05 g) was carried out at 423 K. The H_2/He mixture ratio was 1 with total flow rate of 100 $cm^3\,min^{-1}$. Gas containing benzene (1 vol% of benzene) was prepared by passage of He stream through a benzene placed in a saturator maintained at 278.4 K.

The kinetic studies on reduced samples (0.05 g) were carried out in the temperature range of 348–423 K with low benzene conversion (lower than 10%).

3. Results and discussion

3.1. Reduction of the supported Ni^{2+} ions in the hydrazine media

The green colour of impregnated monometallic Ni changed to blue, ascribed to formation of $[Ni(N_2H_4)_3]^{2+}$ complex [34,40] then to dark due to colloidal Ni^0 production. In contrast, green impregnated Ni–Ag catalysts directly changed to dark due to fast Ag^+ and Ni^{2+} ions reduction. Indeed, the Ag added metal is very easily reduced and the Ag^0 metal particles formed play the role of active centers for nickel reduction. It has been shown that silver ions added to the reactant mixture accelerated the reduction of transition metals ions [41]. Presence of Ag_2O also improved reduction of supported nickel oxide with hydrogen [38,39,42].

For the Ni or Ni–AgPC precipitated catalysts, the reduction solution transitorily became blue before it turned to dark, the colour of colloidal Ni^0. The changes observed are also ascribed to formation of $[Ni(N_2H_4)_3]^{2+}$ complex which next is reduced in the solution or in the vicinity of the silica support, allowing Ni^0 particles to precipitate on the surface.

For impregnated catalysts one expects that some amount of acetate or nitrate metal precursors may desorb in the hydrazine media then precipitate and this could influence on the properties of the final materials. However that may be, the results obtained clearly show that surface and catalytic properties of impregnated and precipitated catalysts are quite different.

3.2. Physical characterization

XRD patterns of the pure Ni, Ag and Ni–Ag particles recorded (not shown). Well crystallized metallic particles were obtained. Weaker metallic signals were found with metal supported materials. Typical spectra are given in Fig. 1.

The peaks of nickel and silver metallic particles with fcc structure [43] were detected for monometallic catalysts, respectively. The intensity of the (111) silver peak at 38.116 increases as the silver content in the catalyst increases. The (111) characteristic peak at 44.599 for metallic nickel was almost not detected. No Ni–Ag alloys were detected. The absence of a signal or the existence of a very weak signal could confirm a high dispersion of nickel active phase or express low nickel content in the catalysts.

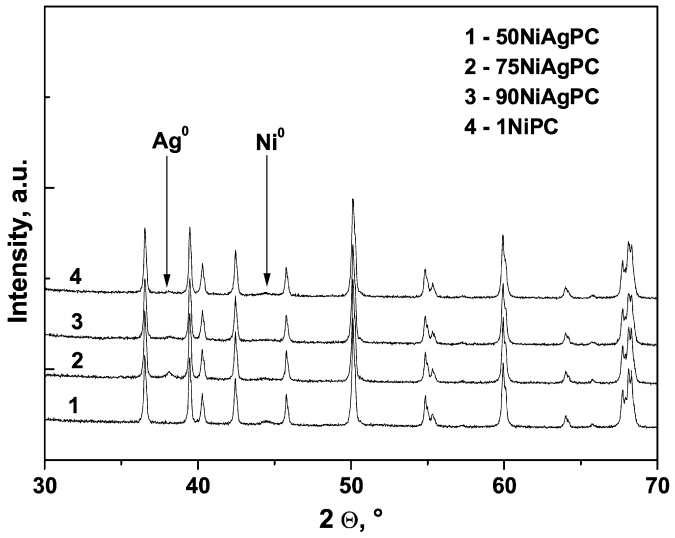

Fig. 1. XRD patterns of the precipitated catalysts.

STEM images and X-mapping analysis were recorded for 1NiIC, 50NiAgIC and 75NiAgPC catalysts. Typical results are reported in Fig. 2. The EDXS analysis confirmed the presence of the nickel and silver on the support. The particles were found as Ni, Ag or Ni–Ag crystallites. In bimetallic crystallites Ni and Ag were as segregated phases with a Ni/Ag ratio of 1. In case of the monometallic 1NiIC catalyst the TEM image showed the presence of fiber-like nickel particles (not shown). The particle size range was 8–30 nm for both monometallic and bimetallic Ni–Ag phases. Nickel appears as more dispersed in bimetallic NiAg than monometallic Ni for precipitated catalysts. The reverse is observed for impregnated catalysts.

The results obtained are in agreement with the literature data. Indeed, nickel and silver do not form stable solid solutions. Metastable NiAg alloys have been observed in specific conditions [21,22]. These metastable alloys give rise to phase separation and reformation of Ni and Ag particles with time on stream [21]. Only few studies were devoted to supported NiAg systems as catalysts [38,39]. In case of $NiAg/SiO_2$, XRD and EXAFS study showed no influence of silver on the bulk structure of nickel, that is Ni and Ag were as separate phases [38].

3.3. Degree of reduction

The degree of reduction was determined by the oxygen chemisorption after a hydrogen treatment according to a previous procedure [27]. The results are reported in Table 1. The values reported comprise total metal (Ni + Ag) reduction.

All catalysts were highly reduced (above 79%). In the presence of silver the degree of reduction strongly increases, to a higher extent with precipitated (79.4–100.0%) than with impregnated (81.1–93.9%) catalysts. At high content (0.50%) the degree of reduction strongly increases, up to 93.9 or 100% for impregnated or precipitated catalysts, respectively. At the low silver content of 0.1% there no almost change in the degree (around 80%).

The values of degree of reduction here reported in Table 1 have been determined after a standard pre-treatment of the

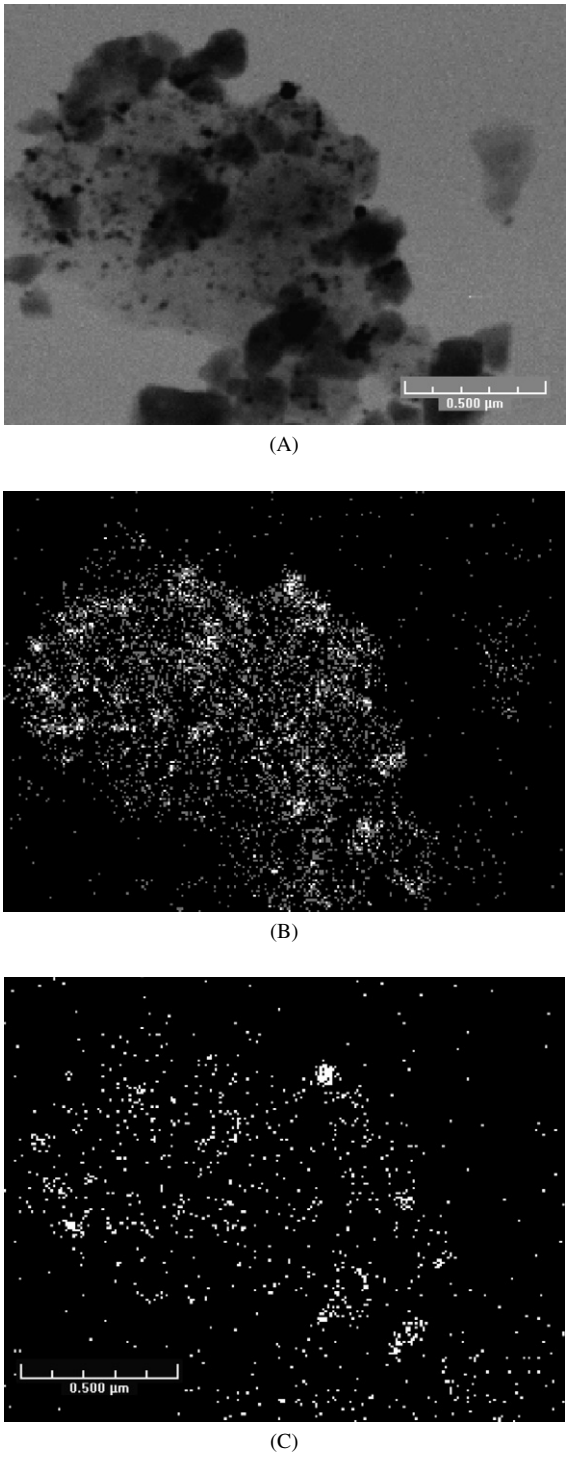

Fig. 2. 75NiAgPC catalyst: STEM image (A) and X-mapping analysis for Ni (B) and Ag (C) components.

freshly prepared catalysts (see Section 2). It can be seen that they depend to some extent on method of preparation and Ni/Ag ratio. They reflect the structural and chemical properties of the nanoparticles formed in the hydrazine media. In this media, silver rapidly form Ag^0 species which serve as active centers for nickel reduction which therefore is accelerated. The extent of the reduction may be related to the chemical processes involved. These processes are discussed below.

Table 1
Characteristics of catalysts prepared

Catalyst	Ni (wt%)	Ag (%)	H_2 ads $\times 10^{-5}$ ($mol_{H_2}\ g_{cat}^{-1}$)	H_2 des[a] $\times 10^{-5}$ ($mol_{H_2}\ g_{cat}^{-1}$)	Degree of reduction (%)	Dispersion (%)	Ni particle size[b] (nm)	Ni + Ag (%)
1NiPC	1.16	–	0.34	0.76	82.4	5.5	18.2	1.16
90NiAgPC	0.87	0.13	0.27	0.29	79.4	5.5	18.2	1.00
75NiAgPC	0.72	0.28	0.63	0.38	85.4	13.3	7.5	1.00
50NiAgPC	0.46	0.47	0.29	0.22	100	6.7	14.8	0.93
1NiIC	1.23	–	0.50	1.31	81.1	8.9	11.2	1.23
90NiAgIC	0.80	0.12	0.37	1.16	82.8	7.1	14.3	0.92
75NiAgIC	0.76	0.28	0.27	1.38	82.7	6.4	15.7	1.04
50NiAgIC	0.45	0.47	0.22	1.19	93.9	4.6	22.0	0.92
1AgIC	–	1.06	0.00	0.00	82.4	5.5	18.2	1.06

[a] From H_2 TPD experiments.
[b] From H_2 adsorption experiments.

The results obtained are in agreement with the scarce studies reported in the literature on the reducibility of supported NiAg oxides classically prepared. Indeed, H_2-TPR studies showed that presence of the silver decreased temperature of reduction of the nickel supported on SiO_2 [38] or zeolites [39]. It is assumed that silver oxide is first reduced at low temperatures to form silver atoms on which H_2 molecules dissociates to highly reductive H atoms: these atoms are responsible of the reduction of the nickel at the lower temperatures observed.

3.4. H_2 adsorption

Hydrogen adsorption at room temperature was used for the study of metal surface area. Average metal particle size and dispersion were then calculated. The results are shown in Table 1.

As expected [28,29,44], silver does not adsorb hydrogen at room temperature. For monometallic catalysts, better dispersion is obtained by impregnation (7.2%) than by precipitation (4.5%) method. The reverse is observed for bimetallic systems: higher dispersion is obtained with precipitated catalysts than with impregnated catalysts. Moreover, in bimetallic systems, the dispersion decreases with increasing silver content for impregnated catalysts but passes through a maximum for precipitated catalysts. The 75NiAgPC catalyst exhibits the highest dispersion of 11.4% and the lowest particle size of 8.8 nm.

The mechanism of metal particle formation consists in two steps: nucleation and particle growth. In order to obtain monodisperse particles a first general condition must be fulfilled: nucleation and growth must be two completely separated steps [41]. In case of the bimetallic catalysts preparation the heterogeneous nucleation can be achieved by forming in situ seed particles before the nucleation take place [41]. The difference in the observed catalyst properties arose from the difference in the number of nuclei formed and the growth rate. This difference here depends on the reduction conditions (precipitation/impregnation) and the metal chemical composition. Nucleation and growth mainly took place on the support for impregnated catalysts and in the solution or in the vicinity of the support for precipitated catalysts. Ag^0 metal particles are readily formed and play the role of active centers for nickel reduction. Hence increasing Ag^+ content increases the number of nuclei formed and nickel reduction rate.

For the impregnated IC catalysts, metal dispersion is already determined in the impregnation step. Ag^0 metal particles are readily formed and play the role of active centers for nickel reduction. As to the growth processes of the metal nuclei formed, it is expected to occur through surface diffusion for almost all the nuclei formed. In other words, the final size would be determined by the primary metal particles formed. Also, from the above considerations, the decrease of dispersion with increasing Ag content for impregnated catalysts suggests that the nucleation and reduction of the metal nanoparticles occur simultaneously in the presence of silver. This leads to the quick growth of nanoparticles.

For precipitated catalysts one can speculate the existence of a great number of homogeneously distributed Ag^0 centers in solution on which nickel ions are readily reduced. Reduced silver particles form tiny metallic particles acting as foreign nuclei for subsequent growth of nickel particles. This could explain the increase of metal dispersion with increasing the silver content for precipitated catalysts up to a maximum. More silver ions introduced to the reactant mixture more silver nuclei for nickel particles growth. Above maximum, excess silver ions probably induces a faster particle growth which decreases the dispersion.

Whatever the process of formation of the nanoparticles, in the precipitated bimetallic system, there exist a specific Ni and Ag atoms groupings which arrange so as to expose a greater number of surface Ni atoms than in the monometallic system. Moreover, one has to get in mind that Ni and Ag do not form stable alloys [21,22]. Therefore, we may infer that some metastable supported NiAg alloy, of high metal surface area, arose in the hydrazine media but were not detected by the tools we used to characterize the catalysts. More refined analyzes are required to confirm the existence of these arrangements. As a matter of fact, a sharp increase in the surface and catalytic performances of supported nickel phase is observed in the presence of silver metal additive for the hydrazine catalysts. This has not been reported before in the literature.

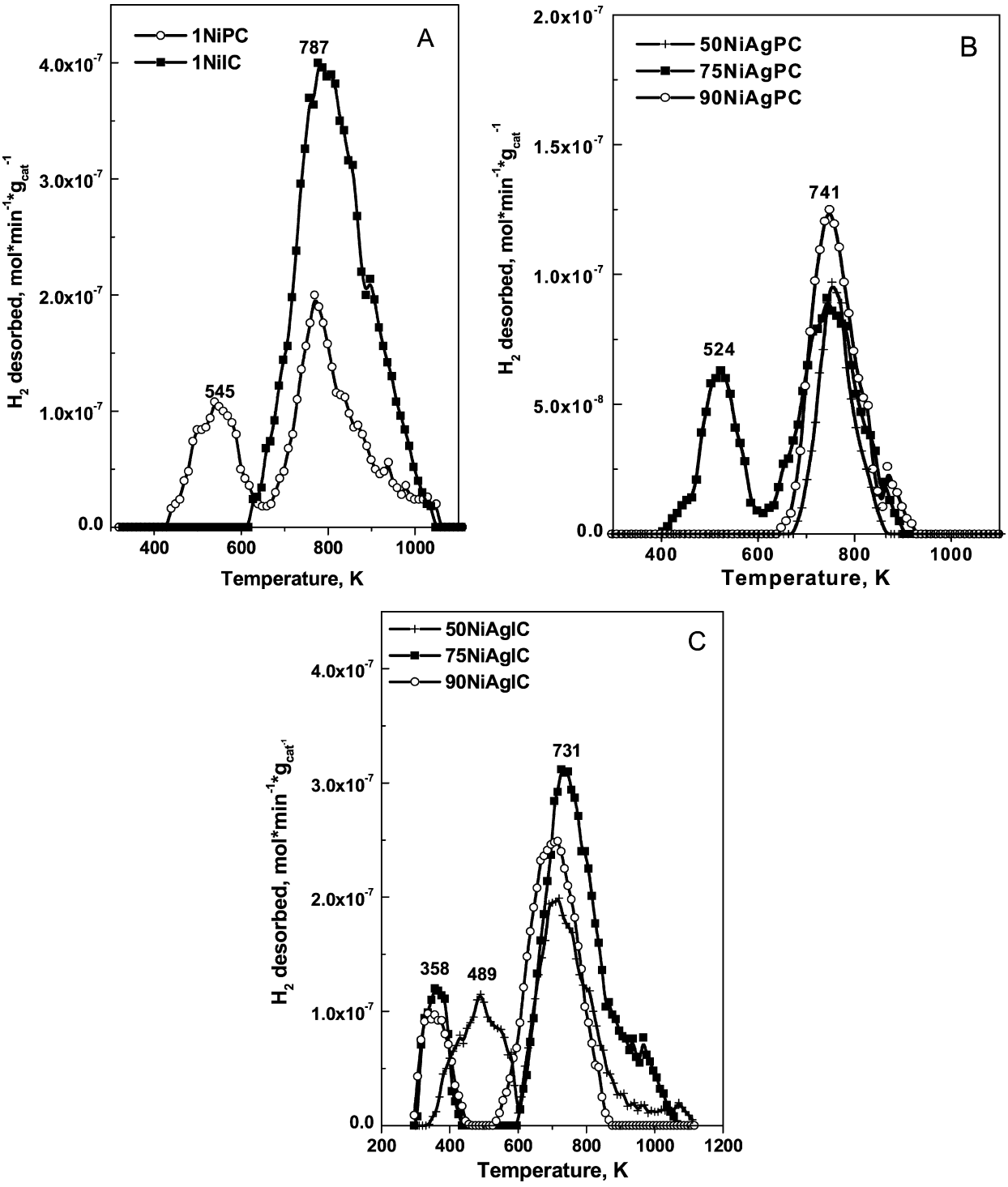

Fig. 3. H_2-TPD profiles of the nickel monometallic catalysts (A) and precipitated (B) or impregnated (C) bimetallic catalysts.

3.5. H_2 TPD studies

The H_2 TPD experiment results are shown in Fig. 3 and Table 1.

The catalysts exhibit two main domains of desorption in low (<600 K) and high (>600 K) temperature ranges, respectively. The first domain corresponds to hydrogen weakly adsorbed on the nickel surface whereas the second could originate from much more strongly adsorbed hydrogen, probably at the metal–support interface or on the support as spilt-over species [45,46].

Monometallic catalysts exhibit same high temperature peak at 787 K but the low temperature (545 K) appears only for the precipitated catalyst (Fig. 3A). The presence of silver decreases maximum temperature peaks to 741 and 524 K, respectively, for precipitated catalysts (Fig. 3B). For impregnated catalysts silver also decreased maximum temperature peak to 741 K for (Fig. 3C) and, in addition, induced ap-

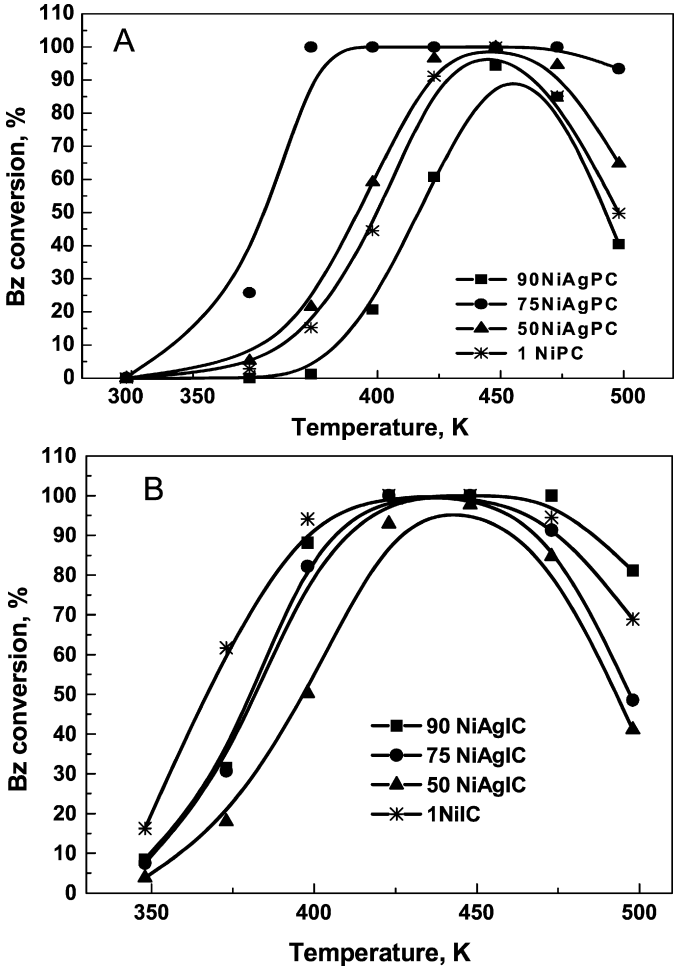

Fig. 4. Benzene conversion versus temperature of reaction for precipitated (A) and impregnated (B) catalysts.

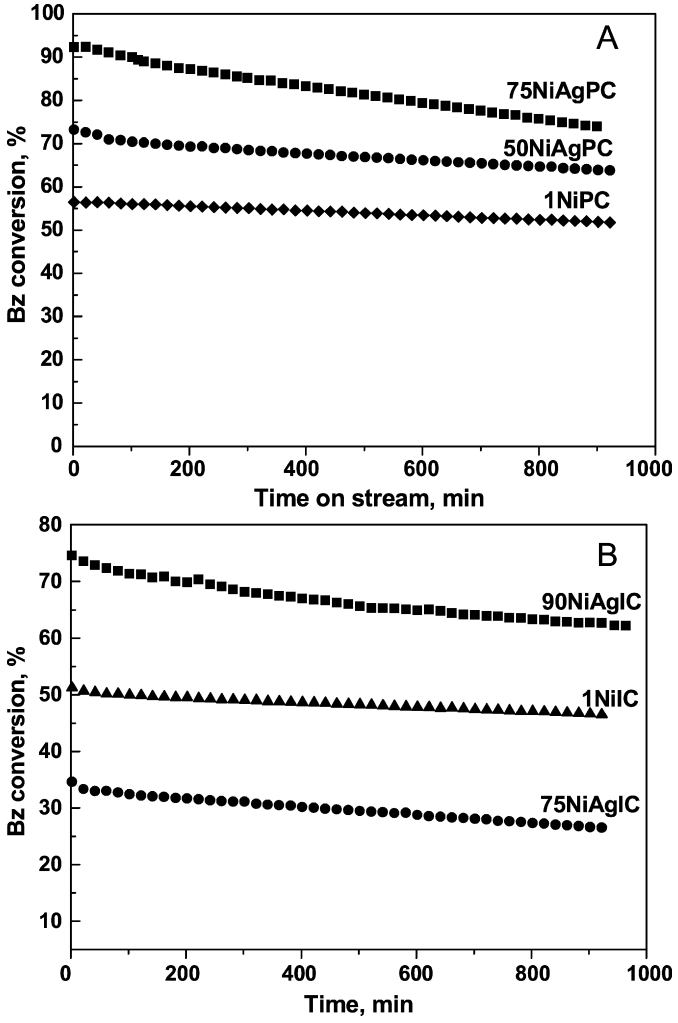

Fig. 5. Benzene conversion versus time of stream for precipitated (A) and impregnated (B) catalysts.

pearance of low temperature peaks at 358 and 489 K, respectively.

It is worth noting that impregnated catalysts desorb higher amounts of hydrogen than they adsorb at room temperature. The excess hydrogen desorbed may be ascribed to the hydrogen molecules retained on the catalyst during the heat pre-treatment at 573 K under flowing hydrogen. These molecules, trapped at high temperatures, are strongly adsorbed, probably at the metal–support interface or on the support as spilt-over species [45,46]. In contrast, precipitated catalyst desorb less hydrogen than impregnated catalysts. Moreover, hydrogen uptake at high temperature is lower than that at room temperature, notably for 75NiAgPC (3.8 against 6.3 μmol g_{cat}^{-1}, Table 1). Hydrogen lack is mostly due to loosely attached molecules desorbing during the purging at room temperature before the TPD experiments started (see Section 2).

3.6. Catalytic activity

The gas phase hydrogenation of benzene was used as a catalytic test for prepared catalysts. All the catalysts showed 100% selectivity to cyclohexane. The bare supports do not exhibit catalytic activity in this reaction. The results obtained are reported in Figs. 4–6 and Table 2.

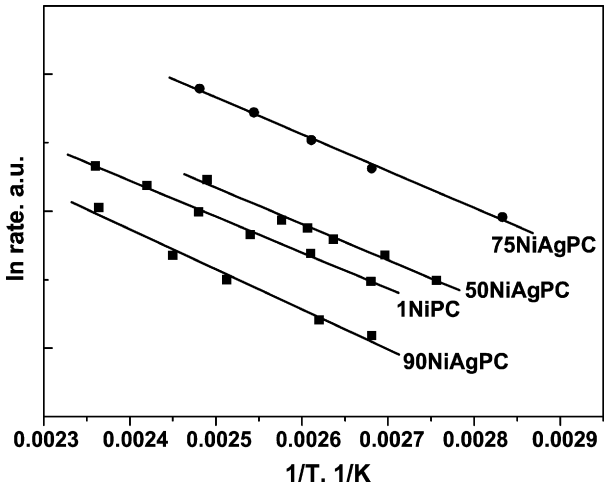

Fig. 6. Arrhenius plots for precipitated catalysts.

The results obtained show that the catalytic activity is determined by the method of preparation and Ni/Ag ratio. Silver

Table 2
Conversion, TOF's and energy of activation in benzene hydrogenation for the SiO_2(C) supported catalysts at 373 and 448 K

Catalyst	Benzene conversion (%)		TOF $\times 10^{-3}$ (molecule Bz s^{-1} $site^{-1}$)		Activation energy (kJ mol^{-1})
	348 K	373 K	348 K	373 K	
1NiPC	2.8	15.2	11	59	44.6
90NiAgPC	0	1.2	0	7	41.7
75NiAgPC	25.8	100	61	–	39.6
50NiAgPC	5.2	21.5	28	115	39.5
1NiIC	16.2	61.7	39	149	38.2
90NiAgIC	8.4	31.4	36	136	44.4
75NiAgIC	7.5	30.7	39	163	43.2
50NiAgIC	3.8	17.9	28	132	40.6

monometallic catalysts were inactive. Monometallic nickel and NiAg bimetallic catalysts exhibited a maximum of activity as a function of the reaction temperature (Fig. 4). The temperature of this maximum depends on the method of preparation of the catalysts and nature of the support. This maximum is accounted for a positive influence of the reaction kinetics at lower temperatures whereas, at higher temperatures, the thermodynamic effect of the reaction was prevailing and then conversion decreased [47]. The maximum of activity is also attributed to a decrease of the surface coverage by benzene molecules at the higher temperatures [48,49].

The most important feature of the results obtained is improvement of nickel activity in the presence silver for precipitated catalysts: the maximum activity is observed at much lower reaction temperature (350 K) than in the absence of silver (450 K). This synergistic effect has not been reported before.

For monometallic catalysts, impregnation is better than precipitation method (conversions at 348 K are 16.2 and 2.8%, respectively). In contrast, for bimetallic catalysts, precipitation is the best method: the conversion is total from 373 K for the former and only from 413 K for the impregnated catalysts. At 373 K the conversion hardly reaches 30% for the latter catalysts. The effect of the silver content strongly depends on the method of preparation. 75NiAgPC is the most active catalyst. Remarkably, this catalyst showed catalytic activity at room temperature which is not common for nickel catalysts. This is ascribed to combined effect of method of preparation and presence of a second metal.

The use of the turnover frequencies (TOF's) allows one to make a valuable comparison of the intrinsic activity of the nickel surface atoms. The results obtained at 348 K are reported in Table 2. The TOF's values obtained follow the metal dispersion variations for precipitation method A very high TOF is obtained for 75NiAgPC catalyst: 0.061 s^{-1} which is 6 times greater than that of monometallic precipitated catalyst. Silver additive does not influence the intrinsic reactivity of nickel for impregnated catalysts since almost same TOF's are obtained (around 0.035 s^{-1}). The method of preparation not only determine the extent of the metal surface area but also its structural properties, notably in presence of the silver.

It is worth noting that the TOF value observed at 348 K (0.233 s^{-1}) is higher than the standard values reported for nickel catalysts (0.005–0.033 s^{-1}) [34,50] and close to that obtained for platinum catalysts at 333 K (0.033–0.078 s^{-1}) [24].

The stability of the catalysts was tested at 373 K for 16 h. Typical results are given in Fig. 5. Monometallic catalysts were almost stable with time on stream. In contrast, bimetallic catalysts exhibited some deactivation. This effect is more pronounced for precipitated catalysts. This effect is due to the negative processes occurring during the hydrogenation reaction. Poisoning of active centers by the coke formation has also to be considered. It would also be due to some structural modification of the catalysts since, as discussed above, Ni and Ag elements could form metastable bimetallic systems which evolve with time on stream to phase separation.

The apparent energy of activation was determined at 248–423 K in kinetic regime (at conversions <10%). The results obtained are reported in Fig. 6 and Table 2. The values obtained are in the lower range of published results for SiO_2 supported catalysts (>50 kJ mol^{-1}) [51]. They changed with the method of preparation and silver content. For monometallic catalysts the apparent energy of activation is lower for impregnated 1NiIC catalyst (38.2 against 44.6 kJ mol^{-1}). In contrast, for bimetallic catalysts, apparent energy of activation is roughly lower for precipitated catalysts (39.6–41.7 kJ mol^{-1} against 40.6–44.4 kJ mol^{-1}). This is in agreement with the relative activity of these catalysts, notably above 373 K (Figs. 4–5). Moreover, recall that above TPD study evidenced the existence of weak H_2 adsorption sites for Ni–Ag precipitated. On such sites, adsorbed hydrogen species are more reactive and this could explain a lower apparent energy of activation and a higher activity.

4. Conclusions

The present study showed that the NiAg/SiO_2 system consisted in both Ni and Ag monometallic nanoparticles and bimetallic NiAg nanoparticles with segregation of Ni and Ag phases. The investigation also showed that surface properties and reducibility of catalysts prepared strongly depend on the mode of reduction by the hydrazine and the Ni/Ag ratio.

The most important feature of the results obtained is the improvement of the dispersion and the catalytic activity of nickel in the presence silver in case of precipitated catalysts. This synergistic effect between Ni and Ag has not been reported before. This result is remarkable since supported Ag is not active toward hydrogen or in the hydrogenation reaction. Dispersion and activity pass through a maximum or monotonically decrease with precipitated and impregnated catalysts respectively with increasing Ag content. 75NiAgPC catalyst exhibits the highest dispersion of 11.4% and the lowest particle size of 8.8 nm. It gives rise to total conversion from 373 K, a temperature at which conversion hardly reaches 30% for the other catalysts. Deactivation was observed for bimetallic catalysts, particularly with precipitated samples.

These results could be explained by the mechanism of metal reduction in the hydrazine media. For the supported IC systems, nucleation and growth probably mainly took place on the support whereas for the precipitated PC catalysts, the metal reduction mostly occurred in the liquid phase. In the presence of

silver, Ag^0 clusters first formed and served as active centers for nickel subsequent reduction. As a result, various Ni–Ag species formed where Ni and Ag phases were separated clusters or interacted as heteroatomic groupings on the carrier surface. These grouping would be responsible of the high performances of the precipitated catalysts.

References

[1] B.F.G. Johnson, Top. Catal. 24 (2003) 147.
[2] S. Panigrahi, S. Kundu, S.K. Ghosh, S. Nath, T. Pal, J. Nanopart. Res. 6 (2004) 411.
[3] S.I. Dolgaev, A.V. Simakin, V.V. Voronov, G.A. Shafeev, F. Bozon-Verduraz, Appl. Surf. Sci. 186 (2002) 546.
[4] A. Pal, K. Esumi, T. Pal, J. Colloid Interface Sci. 288 (2) (2005) 396.
[5] D. Wang, C. Song, Z. Hu, X. Zhou, Mater. Lett. 59 (2005) 1760.
[6] Y.H. Kim, D.K. Lee, Y.S. Kang, Colloids Surf. A 257–258 (2005) 273.
[7] H. Wang, X. Qiao, J. Chen, S. Ding, Colloids Surf. A 256 (2005) 111.
[8] K.H. Kim, H.C. Park, S.D. Lee, W.J. Hwa, S.S. Hong, G.D. Lee, S.S. Park, Mater. Chem. Phys. 92 (2005) 234.
[9] Y. Duan, J. Li, Mater. Chem. Phys. 87 (2004) 452.
[10] D.H. Chen, C.H. Hsieh, J. Mater. Chem. 12 (2002) 2412.
[11] Y. Hou, H. Kondoh, T. Ohta, S. Gao, Appl. Surf. Sci. 241 (2005) 218.
[12] K.N. Kim, S.G. Kim, Powder Technol. 145 (2004) 155.
[13] M. Seipenbusch, A.P. Weber, A. Schiel, G. Kasper, Aerosol Sci. 34 (2003) 1699.
[14] Y.V. Bokshits, G.P. Shevchenko, A.N. Ponyavina, S.K. Rakhmanov, Colloid J. 66 (5) (2004) 517.
[15] Y. Kobayashi, S. Kiao, M. Seto, H. Takatani, M. Nakanishi, R. Oshima, Hyperfine Interact. 156/157 (2004) 75.
[16] A. Henglein, J. Phys. Chem. B 104 (2000) 2201.
[17] X. Su, H. Zheng, Z. Yang, Y. Zhu, A. Pan, J. Mater. Sci. 28 (2003) 4581.
[18] Y.D. Li, L.Q. Li, H.W. Liao, H.R. Wang, J. Mater. Chem. 9 (1999) 2675.
[19] C.H. Jung, H.G. Lee, C.J. Kim, S.B. Bhaduri, J. Nanopart. Res. 5 (2003) 383.
[20] S.Y. Yang, S.G. Kim, Powder Technol. 146 (2004) 185.
[21] A. Kumar, Ch. Damle, M. Sastry, Appl. Phys. Lett. 79 (20) (2001) 3314.
[22] D. Poondi, J. Singh, J. Mater. Sci. 35 (2000) 2467.
[23] T. Bala, A. Swami, B.L.V. Prasad, M. Sastry, J. Colloid Interface Sci. 283 (2005) 422.
[24] S.D. Lin, M.A. Vannice, J. Catal. 143 (1993) 539.
[25] M. Houalla, B. Delmon, J. Phys. Chem. 84 (1980) 2194.
[26] S.P. Noskova, M.S. Borisova, V.A. Dzisko, Kinet. Katal. 16 (2) (1975) 497.
[27] C.H. Bartholomew, R.J. Farrauto, J. Catal. 45 (1976) 41.
[28] J.J.F. Scholten, J.A. Konvalinka, F.W. Beekman, J. Catal. 28 (1973) 209.
[29] S.R. Seyedmonir, D.E. Strohmayer, G.L. Geoffroy, M.A. Vannice, H.W. Young, J.W. Linowski, J. Catal. 87 (1984) 424.
[30] Q. Zhang, J. Li, X. Liu, Q. Zhu, Appl. Catal. A Gen. 197 (2000) 221.
[31] H.K. Kim, Y.B. Lee, E.Y. Choi, H.C. Park, S.S. Park, Mater. Chem. Phys. 86 (2004) 420.
[32] S.H. Wu, D.H. Chen, J. Colloid Interface Sci. 259 (2003) 282.
[33] H.T. Zhang, Y.M. Xiong, X.G. Luo, C.H. Wang, S.Y. Li, X.H. Chen, J. Cryst. Growth 242 (2002) 259.
[34] A. Boudjahem, S. Monteverdi, M. Mercy, M.M. Bettahar, Langmuir 20 (2004) 208.
[35] A. Degan, J. Macek, Nanostruct. Mater. 12 (1999) 225.
[36] U. Nickel, A.Z. Castell, P. Karin, S.A. Schneider, Langmuir 16 (2000) 9087.
[37] M. Pietrowski, A.-G. Boudjahem, M.M. Bettahar, J. Mater. Sci. 41 (2006) 2025.
[38] G. Ertl, H. Knözinger, J. Weitkemp (Eds.), Handbook of Heterogeneous Catalysis, vol. 2, VCH, Weinheim, 1997, p. 439.
[39] F. Dorado, A. de Lucas, P.B. Garcia, A. Romero, J.L. Valverde, I. Ascencion, Ind. Eng. Chem. Res. 44 (2005) 8988.
[40] A. Jasik, R. Wojcieszak, S. Monteverdi, M. Ziolek, M.M. Bettahar, J. Mol. Catal. A Chem. 242 (2005) 84.
[41] J.T. Richardson, B. Turk, M. Lei, K. Forster, M.V. Twigg, Appl. Catal. A Gen. 83 (1992) 87.
[42] G. Viau, F. Fievet-Vicent, F. Fievet, Solid State Ionics 84 (1996) 259.
[43] 999 JCPDS Inter. Centre for Diff. Data.
[44] S.R. Seyedmonir, D.E. Strohmayer, G.J. Guskey, G.L. Geoffroy, M.A. Vannice, J. Catal. 93 (1985) 288.
[45] W.C. Conner, J.L. Falconer, Chem. Rev. 95 (1995) 759.
[46] U. Roland, T. Braunschweig, F. Roessner, J. Mol. Catal. A Chem. 127 (1997) 61.
[47] P. Antonucci, N. Van Truong, N. Giordano, R. Maggiore, J. Catal. 75 (1982) 140.
[48] I. Ionnanides, X.E. Verykios, J. Catal. 143 (1993) 175.
[49] S.D. Lin, M.A. Vannice, J. Catal. 143 (1993) 563.
[50] M. Houalla, F. Delannay, B. Delmon, J. Chem. Soc. Faraday Trans. 76 (1980) 2128.
[51] R. Molina, G. Poncelet, J. Catal. 199 (2001) 162.